ELSEVIER

On the relation between oxygen diffusion and secondary relaxation in glassy *n*-butanol

V.M. Syutkin *, B.V. Bol'shakov, A.G. Dzhonson

Institute of Chemical Kinetics and Combustion, Institutskaya, 3, Novosibirsk 630090, Russian Federation

Abstract

The kinetics of *tert*-butyl radical oxidation by molecular oxygen in glassy *n*-butanol has been studied over the temperature range of 77–101 K. It is shown that the rate constant of the decay of radicals depends on their location, i.e. the radical oxidation kinetics is spatially heterogeneous. This kinetics has been discovered to become more homogeneous with increasing reaction temperature without any glass restructuring. We assign this to the activation of the degrees of freedom responsible for secondary relaxation, which makes glass more homogeneous with respect to oxygen diffusion.

The temperature dependence of target problem in a medium with energy disorder has been evaluated by computer simulation in the framework of the random barrier model. A box distribution of barrier heights was used. The temperature was varied from $T^*/40$ to $T^*/20$, where T^* is the width of distribution in temperature units. It is shown that the kinetics of target decay is spatially heterogeneous. The number of available pathways remains almost the same with temperature variations.
© 2005 Elsevier B.V. All rights reserved.

Keywords: Organic glasses; Oxygen diffusion; Secondary relaxation; The random barrier model; Target problem

1. Introduction

In supercooled organic liquids, the particles as large as a matrix molecule diffuse with a measurable rate only at temperatures near and above the glass transition temperature T_g (see, e.g. [1]). The matter is that the diffusion of these particles requires molecular rearrangements, which slow down precipitously with glass transition. Below T_g, only small foreign molecules (like the oxygen ones) conserve their diffusion mobility. More likely, their diffusion is determined by lots of cavities of the atomic scale of length (see, e.g. [2]). The cavities are the location for diffusing particles. The diffusion occurs via thermally activated hopping processes over potential barriers between the neighboring cavities. The structural disorder leads to the fact that the barriers between the various pairs of neighboring cavities

are of different height and, as a result, the jump rate of particles varies in space by many orders of magnitude. As a consequence the frequency of the encounter of walking particles with some target can depend on its location.

The non-equivalence of targets can take place, even when the average distance to be covered by mobile particles to encounter a target, is several tens of angstroms. The matter is that every pathway which leads to a target, is always terminated on this target. Therefore, it is impossible to average a difference in the nearest environment of targets.

It is generally believed that in annealed glasses below T_g a potential landscape for mobile particles is "frozen". Thus, of interest are the data of [3].

The kinetics of the oxidation of *tert*-butyl radicals by molecular oxygen has been studied recently in glassy *n*-butanol [3]. The reaction temperature was varied from 87 to 102 K. Note that T_g of *n*-butanol is 114 K [4]. Radicals are used as targets because their decay is controlled by diffusion of oxygen molecules. The reaction in excess oxygen

---
* Corresponding author. Tel.: +73833333456; fax: +73833307350.
  E-mail address: syutkin@ns.kinetics.nsc.ru (V.M. Syutkin).

is a pseudomonomolecular process and its kinetics in a homogeneous medium follows the exponential law.

In glassy *n*-butanol, the radical oxidation kinetics was found to be non-exponential and the kinetic law is a temperature function [3]. The lower the reaction temperature, the stronger is the difference between the radical decay kinetics and the exponential law.

The temperature dependence of the kinetic law can arise for various reasons. First of all, note a trivial reason. Any medium with energy disorder looks more homogeneous with increasing temperature. Another reason is the temperature dependence of glass structure. In this case, a potential landscape for mobile particles is a function of temperature. In addition, the temperature dependence of the kinetic law can arise from unconventional sources based on the undiscovered dynamic processes in glasses.

In this paper, we discuss a cause of the experimentally observed temperature dependence of oxygen diffusion pathways in glassy *n*-butanol.

2. Experimental

To remove water, *n*-butanol of purity 98% was first boiled for 2 h with calcium oxide and then subjected to fractional distillation. The fraction with a boiling temperature of 117.5 °C was used. 1.3 mol% of *tert*-butyl chloride as a precursor of *tert*-butyl radicals and 10^{-3} mol/l of diphenylamine (DFA) as an electron donor were added to *n*-butanol.

The quartz ampoules with 3 mm i.d. were used. In the upper part of the ampoule there was a special compartment to saturate liquid with gas [5]. Solution was saturated either with oxygen or with an oxygen–nitrogen mixture at room temperature. The Henry constant is 5.2×10^{18} cm^{-3} amt^{-1} for oxygen and 3×10^{18} cm^{-3} amt^{-1} for nitrogen [6]. The oxygen concentration in solution was varied from 10^{18} to 5×10^{19} cm^{-3} by changing the partial oxygen pressure over liquid in the ampoule from 0.2 to 9.6 atm. The partial nitrogen pressure was chosen so that the total concentration of gas molecules in solution was no less than 3.2×10^{19} cm^{-3}. The gas-saturated solution was poured from compartment to the lower part of the ampoule without disconnecting it from the gas-cylinder. The height of the sample was about 7 cm. Solution was frozen by dipping first the lower part of the ampoule (about 5 cm in height), and 30–40 s later, the remaining part, into liquid nitrogen. This procedure prevents oxygen exchange between the unfrozen part of the sample and the gas phase. We measured the radical oxidation only in the bottommost part of the sample which was 1.5 cm high.

At times, the glass was transparent with a small number of cracks. At other times, it had been first transparent and then it cracked and looked like the compacted powder. It is worth noting that the radical oxidation kinetics was independent of sample appearance. At the same time, the reaction in several samples was 1.5 times as slow as that observed in most cases. Such samples were rejected.

tert-Butyl radicals in glassy *n*-butanol were produced photochemically at 77 K by the following reactions

$$2h\nu + \text{DFA} \rightarrow \text{DFA}^+ + e^-$$

$$(\text{CH}_3)_3\text{CCl} + e^- \rightarrow (\text{CH}_3)_3\dot{\text{C}} + \text{Cl}^-$$
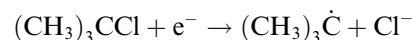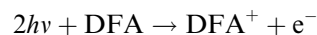
A high-pressure mercury lamp of a power of 1 kW (DRSh-1000) was used as a light source. The light was passed through a water filter 10 cm thick. The photolysis has lasted for 20–40 s. In this case, we remained in the linear part of the curve of the accumulation of *tert*-butyl radicals. The matrix radicals are formed in a small proportion (no more than 10%). The concentration of radicals did not exceed 2×10^{17} cm^{-3}. Note that as the time of photolysis increases, the number of *tert*-butyl radicals stops to increase till the entire DFA is destroyed. In this case, the matrix radicals continue to accumulate.

The concentration of radicals in a sample was measured by the ESR method. The ESR spectra were recorded at 77 K using an RE 1306 spectrometer (USSR). The microwave field power and the modulation amplitude were chosen so that the signal distortion was negligibly small. The signal intensity was normalized over the signal intensity of the standard $\text{CuCl}_2 \cdot 2\text{H}_2\text{O}$ sample located in the cavity.

The ESR spectrum of the *tert*-butyl radical consists of 10, rather narrow lines caused by the interaction between an unpaired electron and nine equivalent β-protons (see Fig. 1 in [3]). The outermost lines of the spectrum are not distorted by the spectrum of peroxide radical however they have low intensity. The spectrum line corresponding to the projection of the total nuclear moment, $I_z = 3/2$, was most suitable for measurements. The matter is that where this line is situated, the peroxide radical spectrum is rather flat. Nevertheless, when the number of *tert*-butyl radicals decreases several times, the height of the line corresponding to $I_z = 3/2$ stops to be proportional to the number of *tert*-butyl radicals. A correction should be introduced according to the method proposed [7]. A relative number of
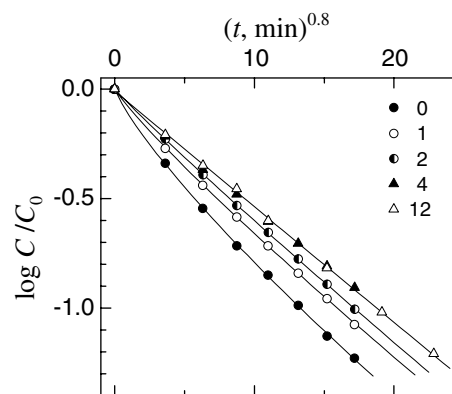

Fig. 1. The influence of *n*-butanol glass annealing at 100 K on the kinetics of *tert*-butyl radicals decay. Reaction temperature is also 100 K. The time of annealing in hours is shown in the legend. The partial oxygen pressure is 1 atm. Lines are guides for the eye.

radicals, $C(t)/C_0$, is equal to the value $(h(t) - h(\infty))/(h(0) - h(\infty))$ where h is the difference in the intensity of ESR spectrum, $I(H_2) - I(H_1)$, at the points of magnetic field H_2 and H_1 for which the intensity of the line corresponding to $I_z = 3/2$ is either maximal and minimal. This equation is valid at any concentration of radicals. At short times, $h(t)$ almost coincides with the height of the line of *tert*-butyl radical. After the reaction, $h(\infty)$ is determined by the peroxide radical only. It is worth noting that $h(\infty) \approx -0.03h(0)$ in the samples in which the oxygen concentration $\leqslant 10^{19}$ cm^{-3}. At the same time $h(\infty)$ increases to $-0.06h(0)$ with increasing oxygen concentration to 5×10^{19} cm^{-3} because with a great amount of oxygen in glass, the yield of *tert*-butyl radicals decreases and the number of resulting peroxide radicals remains constant.

3. Results

3.1. The influence of glass annealing on the kinetics of radical oxidation in glassy n-butanol

To avoid the crystallization of liquid, the glasses were produced by the fast cooling of solution to 77 K. The structure of liquid varies with varying temperature. However, when the liquid is cooled to T_g, molecular rearrangements become so much slower that the structure of medium has no time to find its equilibrium state with a further temperature drop [8–10]. Therefore, the glass is a non-equilibrium solid which is continually relaxing toward a more stable state. The changes occur not only in structure but also in the properties of glass, e.g. in the rate of oxygen diffusion. This makes the reaction kinetics dependent on the thermal history of glass.

We have established that the glass annealing at temperatures near 100 K has effect on the reaction kinetics. Fig. 1 shows the kinetics of radical decay at 100 K in samples annealed at different times at the same temperature. It is seen that the annealing performed for 4 h slows down the reaction. From Fig. 1 we notice that the reaction kinetics does not obey the exponential law even in the glasses whose time of annealing highly exceeds the reaction time. In these glasses the oxygen diffusion remains the same during the reaction. As shown below, the non-exponential reaction kinetics is determined by the kinetic non-equivalence of radicals.

As the temperature decreases, the relaxation rate decreases faster than the reaction rate. We have established that below 95 K the glass annealing during the period which is many times the reaction time, has almost no effect on the kinetics of radical decay.

Fig. 2 shows the influence of the prolonged glass annealing at 101 K on the reaction kinetics at 90 K. It is seen that although the reaction in the annealed glass is slower, the kinetic law remains almost the same. The characteristic reaction time increases by 30–40%. A similar behavior of reaction kinetics is recorded for all oxygen concentrations. Thus, a change in glass structure observed during anneal-
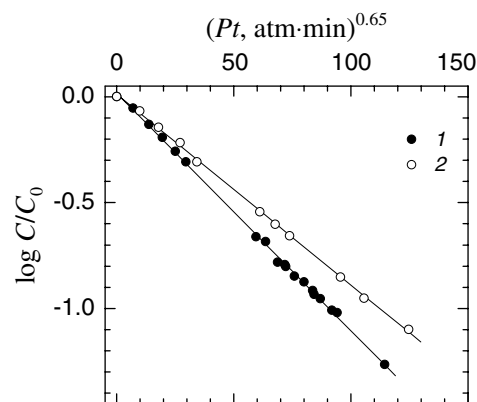

Fig. 2. The kinetics of *tert*-butyl radicals decay at 90 K in *n*-butanol glass without annealing (1) and after annealing at 101 K during 7 h (2). The partial oxygen pressure $P = 0.4$ atm. Straight lines are guides for the eye.

ing at temperatures near 100 K, has no influence on the kinetic law of radical decay.

According to the data in Figs. 1 and 2, the kinetic law of radical oxidation depends on temperature. Indeed, at 90 K the reaction kinetics is well approximated by a fractional exponential with an exponent of 0.65 whereas at 100 K the exponent is 0.8. It should be stressed that the kinetic law changes without any glass restructuring. Indeed, since no relaxation actually occurs at 90 K, the glass structure is the same in both cases. It is formed during prolonged annealing at 100 K.

3.2. The temperature dependence of radical oxidation kinetics in glassy n-butanol

The temperature dependence of radical oxidation kinetics has been studied in glasses first annealed at reaction temperature during the period which is many times the reaction time. This annealing guarantees stationary reaction conditions. According to [11,12], our glasses contain about 10^{18} cm^{-3} of the so-called traps. A microscopic origin of these traps is unknown. In such a trap, an oxygen molecule loses its diffusion mobility and is not actually involved in the reaction. To eliminate the effect of traps on oxygen diffusion in the case of its low concentration, solution was saturated with an oxygen–nitrogen mixture. The total number of gas molecules always exceeded the number of traps by more than an order of magnitude. When the oxygen concentration is low, the nitrogen fills almost all traps to prevent the capture of oxygen.

Fig. 3 shows the kinetics of radical oxidation at different temperatures. First we discuss the decay of radicals as a function of time.

Although the reaction is actually the first-order process, its kinetics cannot be described by the exponential law due to the kinetic non-equivalence of radicals, which follows from the observed dependence of reaction kinetics on oxygen concentrations. When the various subenzembles of
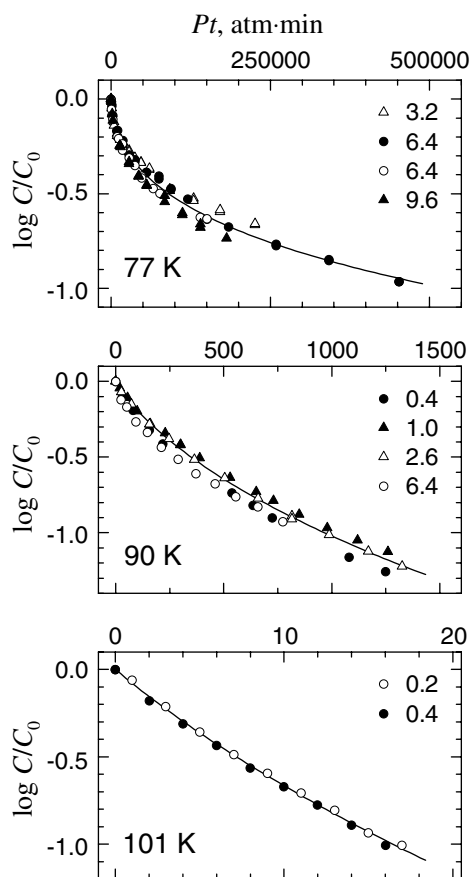
Fig. 3. The kinetics of *tert*-butyl radicals decay in *n*-butanol glass at different temperatures. The partial oxygen pressure, *P*, in atmospheres is shown in the legends. Lines represent approximation of the experimental data by Eq. (1) with $g(k)$ given by Eq. (3).

radicals have different rate constant, the kinetics of radical decay is of the form

$$C(t)/C_0 = \int g(k) \exp(-kPt) \, dk, \qquad (1)$$

where $g(k)$ represents a spatial distribution of rate constant. Since the oxygen concentration, *P*, and the reaction time, *t*, are present in Eq. (1) as co-factors, the result of integration over *k* is a function of *Pt* (first mentioned in [13])

$$C(t)/C_0 = \exp(-F(Pt)). \qquad (2)$$

Thus, when the non-exponential reaction kinetics is determined by rate constant distribution, the data on glasses with different oxygen concentrations should be fitted in the same curve in the coordinates ($\log C/C_0, Pt$). As follows from Fig. 3, this dependence of radical decay kinetics on *P* is observed for our glasses.

The non-exponential reaction kinetics can be also determined by the dependence of the specific reaction rate on time, $k(t)$ (see, e.g. [14]). This, however, provides a sharper dependence of radical decay kinetics on *P* than the rate constant distribution [5,13].

Note that the dependence of oxidation kinetics on oxygen concentration from [3] does not follow Eq. (2). The matter is that the glasses used in [3] contain no nitrogen and as a consequence, the concentration of oxygen participating in the reaction was not equal to the oxygen concentration in the glass [11].

Consider now the temperature dependence of radical oxidation kinetics. Fig. 3 shows that the lower the reaction temperature is, the stronger is the difference between the radical decay kinetics and the exponential law. Thus, the rate constant dispersion increases with decreasing temperature. To qualitatively estimate the temperature dependence of the dispersion, we have used a Gaussian distribution of $\ln k$

$$g(k) \, dk = \frac{1}{\sqrt{2\pi}\sigma} \exp\left(-\frac{(\ln k - \mu)^2}{2\sigma^2}\right) \, d\ln k. \qquad (3)$$

Function (3) has two free parameters: μ and σ. μ is the average value of $\ln k$, and σ is the dispersion of $\ln k$. The solid curves in Fig. 3 are the result of the fit of experimental data to Eq. (1) with $g(k)$ given by Eq. (3). It is seen that the fitted kinetic curves agree satisfactorily with the experimental one. The fitting parameters are in Table 1. As follows from this table, the width of the $\ln k$-distribution function decreases more than three times with increasing temperature from 77 to 101 K.

The temperature dependence of the rate constant can be approximated by the Arrhenius law

$$k(T) = k_0 \exp(-E/RT), \qquad (4)$$

where *R* is the absolute gas constant. The rate constant distribution can arise from both the spatial dispersion of activation energy, *E*, and the spatial dispersion of preexponential factor, k_0. When the latter is a constant, Eq. (4) gives the dispersion of activation energy of σRT. The σRT values at different temperatures are listed in Table 1. It is seen that the dispersion of activation energy, provided the rate constant distribution is determined by activation energy distribution only, decreases 2.5 times with increasing temperature from 77 to 101 K.

It is worth noting that the average value of activation energy, calculated from the temperature dependence of parameter μ, is 6.5 kcal/mol. Referring to Table 1, it exceeds the activation energy dispersion by more than the order of magnitude.

Table 1
The average value and dispersion of $\ln (k, \mathrm{s}^{-1}\,\mathrm{atm}^{-1})$ at different temperatures

T (K)	77	90	101
μ	-16.9 ± 0.2	-10.9 ± 0.15	-6.9 ± 0.1
σ	2.6 ± 0.15	1.22 ± 0.1	0.74 ± 0.1
σRT (cal/mol)	400	220	150

3.3. Monte–Carlo simulation of a target problem in the random barrier model

Any medium with energy disorder looks more homogeneous with increasing temperature. We cannot answer by intuition how sharply the dispersion of rate constant can vary with temperature in such a medium. To understand this we have performed computer simulation of oxygen addition to radicals in the random barrier model. Since the oxygen concentration may be considered as constant in time, the reaction is a special case of the target problem $A + B \rightarrow A$ when only the A particles are mobile [14]. The immobile radicals play the role of targets.

3.3.1. Computational procedure

Computer simulation was performed on a simple cubic lattice consisting of $50 \times 50 \times 50$ sites for mobile particles. Periodic boundary conditions were applied. A site can only be occupied by a single particle. A random number, ϵ, from the range of 0 to T^* is assigned to each bond between the neighbouring sites. This number is considered as the height of the potential barrier in temperature units between these sites. The particle diffusion occurs via the thermally activated jumps over these barriers.

The interstitial space at the center of the lattice is taken as a target (radical). As soon as any mobile particle (oxygen molecule) is at one of the eight sites adjoining the target, the target decay (radical oxidation) is considered to occur.

The reaction was simulated for two oxygen concentrations by taking the number of mobile particles N on the lattice to be 25 and 125. In this case, the fractions of sites, p, occupied by particles are 2×10^{-4} and 10^{-3}, respectively. Let the lattice constant be 3 Å. Thus, for $p = 2 \times 10^{-4}$ the concentration of mobile particles is $7.4 \times 10^{18} \, cm^{-3}$. This value falls in the oxygen concentration range in which the radical oxidation kinetics has been studied.

First, the lattice with a random configuration of barriers is generated and mobile particles are placed in randomly chosen sites. The time is counted from zero. In each elementary step of simulation, a particle and the nearest-neighbour site are randomly chosen. The particle attempts to jump just into this site. If the site is occupied by another particle, the jump is rejected. If the site is vacant, the particle jumps according to the standard Metropolis algorithm with the probability $w = \exp(-\epsilon/T)$, where ϵ is the height of the potential barrier between the sites. After each elementary step, the dimensionless time, t, is increased by $1/N$. The particles walk over the lattice until one of them reaches the site adjoining the target. The time of this event is taken as the time of target decay. Thereafter the simulation is started again from the beginning: a new lattice is generated, and mobile particles are placed over this lattice, and so on. This procedure is repeated $C_0 = 10^4$ times. The number of targets at any given time, $C(t)$, is calculated by subtracting the number of targets decayed at this time from C_0.

3.3.2. Simulation results

The kinetics of target decay differs greatly from the exponential law only at temperatures $\leqslant T^*/20$. In Fig. 4, the plots of $\log C(t)/C_0$ versus pt for $T = T^*/30$ are presented. Clearly, except for short times, the rate of target decay as a function of mobile particle concentration is determined by the pt value only. Thus, the rate constant of the decay of targets depends on their location (see the discussion of Eq. (1)).

It is worth noting that although a medium in the random barrier model is disordered, it is homogeneous. In the model, there is no spatial correlation between barrier heights as in a heterogeneous medium. The kinetic non-equivalence of targets is of purely fluctuation nature.

As seen from Fig. 4, at short times the kinetics of target decay has a sharper dependence on p than that occurs when the kinetic non-equivalence of targets is true. The matter is that a transport of particles in a medium with energy disorder is initially anomalous (see, e.g. [15] wherein the diffusion in the random barrier model has been studied by Monte–Carlo computer simulations). In this case the encounter frequency between mobile particles and a target decreases with time (see, e.g. [16] wherein the target problem in a lattice with randomly removed bonds above the percolation threshold has been studied by Monte Carlo computer simulation). The lower the concentration of mobile particles, the fewer targets decay during the transition from anomalous to normal diffusive mobility. At $p = 2 \times 10^{-4}$, the number of these targets is negligible.

To estimate the temperature dependence of rate constant dispersion, the kinetic curves at $p = 2 \times 10^{-4}$ and $T/T^* = 1/20$, $1/30$, and $1/40$ were approximated by Eq. (1) with $g(k)$ given by Eq. (3). The fitted kinetic curves practically coincide with the experimental one. The fitting parameters are in Table 2.

It is worth noting that the σ value at temperature $T^*/30$ coincides with that found for the reaction of radical oxidation in glassy n-butanol at 96 K.

Recall that the dispersion of activation energy, provided the rate constant distribution is determined by activation
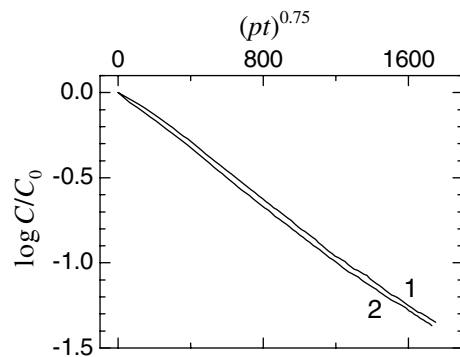

Fig. 4. The kinetics of target decay in the random barrier model at $T = T^*/30$. The fraction of the sites occupied by mobile particles $p = 2 \cdot 10^{-4}$ (1) and 10^{-3} (2).

Table 2
The average value and dispersion of $\ln k$ at different temperatures in the random barrier model

T/T^*	1/40	1/30	1/20
μ	-12.3 ± 0.1	-9.45 ± 0.05	-6.75 ± 0.03
σ	1.26 ± 0.04	0.94 ± 0.02	0.67 ± 0.02
$\sigma \cdot T/T^*$	0.0315	0.0313	0.0335

energy distribution only, varies with temperature as σT (see the discussion of Eq. (4)). As follows from Table 2, the σT value remains almost constant with varying temperature. Let us discuss this result in detail.

Let us assume that the number of available pathways is almost the same over the entire temperature range. Thus, the activation energy of each rate constant is determined by the bottleneck barrier, i.e. the highest barrier which should be overcome by mobile particles to encounter the target. According to our assumption, the spectrum of bottleneck barriers remains unchanged with temperature variations. Thus, the dispersion of activation energies, σRT, should not vary with temperature. As shown above, such behavior of σT holds for our case. Thus, the assumption that the number of available pathways is temperature independent corresponds to the results obtained. We assume this conclusion be valid for a medium with any energy disorder.

The μ value is described satisfactorily by the Arrhenius law with the activation energy $E = (0.274 \pm 0.005)RT^*$. This result may be readily explained in terms of the percolation theory. Indeed, E should actually be close to the average value of the bottleneck barriers which, in turn, should exceed the percolation barrier $\epsilon_p = 0.2488RT^*$ by the value $\approx RT$. The matter is that for a wide distribution of jump rates, the long-range diffusion is limited by barriers within a narrow energy range $\approx RT$ which is higher then the percolation barrier.

4. Discussion

Computer simulation shows that in a medium with energy disorder, the σT value is almost independent of temperature. The matter is that the particles walk practically along the same ways at different temperatures and the dispersion of activation energies is determined by the dispersion of bottleneck barriers. This behavior of activation energies dispersion is inconsistent with the experiment in which σT increases sharply with decreasing temperature (see, Table 1). Thus, the glass studied cannot be considered as a medium in which the effective heights of barriers is temperature independent.

At the same time, a change in barriers with temperature cannot be determined by the temperature dependence of glass structure. Indeed, in the previous Section we have mentioned that no structure relaxation is actually observed at $T < 95$ K. This allowed us to study the reaction kinetics at various temperatures in the glasses whose structure remains unchanged with varying reaction temperature. It has been established that the rate constant distribution changes sharply with temperature without any glass restructuring.

The secondary (Johari–Goldstein) dielectric relaxation is observed in glassy n-butanol over the temperature range in which we have studied the reaction of radical oxidation [4]. The origin of molecular motions that determine this relaxation is not yet clear (see, e.g. Refs. [9,17]). We can be sure only in the fact that a decrease in temperature causes a stepwise deactivation of the subtle degrees of freedom [9]. On the contrary, as the temperature increases, these degrees of freedom are activated. In any case, we are entitled to assert that there are clusters having at last two states that differ in a dipole moment orientation. Transitions between the states (molecular rearrangement of clusters) provide the dielectric response of medium [10]. A characteristic frequency of molecule reorientations, f_p, is temperature dependent and amounts to about 1 kHz at 104 K [4,18]. At this temperature the diffusion coefficient of oxygen molecules is $\approx 10^{-15}$ cm^2/s [12]. Consequently, it can be said with confidence that a jump frequency of oxygen molecules over the bottleneck barriers, v_p, is nearly equal to 1 Hz at 104 K, i.e. v_p is less then f_p by a factor of 1000. The difference in the magnitude of these parameters increases with decreasing temperature as v_p has a sharper dependence on temperature than f_p [4,12].

Let us assume that in various states, the barriers located along the diffusion pathways of oxygen molecules through the cluster are of different heights. Hence, in the temperature range considered here, the energy barriers fluctuate with time, i.e. $\epsilon = \epsilon(t)$. A characteristic frequency of fluctuations is f_p.

We believe that in this case, the number of diffusion pathways increases with temperature, i.e. the glass becomes more homogeneous with respect to oxygen diffusion. Indeed, unfreezing the new degrees of freedom is sure to provide additional possibilities to realize the oxygen molecule jump. This hypothesis will be the subject of future investigations.

References

[1] M.D. Ediger, Annu. Rev. Phys. Chem. 51 (2000) 99.
[2] D.K. Belashchenko, Physics-Uspekhi 42 (1999) 297.
[3] B.V. Bol'shakov, A.G. Dzhonson, J. Non-Cryst. Solids 351 (2005) 444.
[4] S.S.N. Murthy, S.K. Nayak, J. Chem. Phys. 99 (1993) 5362.
[5] V.M. Zaskul'nikov, V.L. Vyazovkin, B.V. Bol'shakov, V.A. Tolkatchev, Int. J. Chem. Kinet. 13 (1981) 707.
[6] V.B. Kogan, V.M. Fridman, V.V. Kafarov, Solubility Handbook, vol. 1, AN SSSR, Moscow, Leningrad, 1962, Book 1, p. 564, 572 (in Russian).

[7] A.A. Stepanov, V.A. Tkatchenko, B.V. Bol'shakov, B.A. Tolkatchev, Int. J. Chem. Kinet. 10 (1978) 637.

[8] M.D. Ediger, C.A. Angell, S.R. Nagel, J. Phys. Chem. 100 (1996) 13200.

[9] C.A. Angell, K.L. Ngai, G.B. McKenna, P.F. McMillan, S.W. Martin, J. Appl. Phys. 88 (2000) 3113.

[10] P.G. Debenedetti, F.H. Stillinger, Nature 410 (2001) 259.

[11] S.V. Vasenkov, V.A. Tolkatchev, J. Chem. Biochem. Kinet. 1 (1991) 357.

[12] B.V. Bol'shakov, V.V. Korolev, V.A. Tolkatchev, J. Struct. Chem. 42 (2001) 220.

[13] V.M. Zaskul'nikov, V.A. Tolkatchev, Kinet. i Katal. 20 (1979) 263.

[14] A. Blumen, G. Zumofen, J. Klafter, in: A. Amann, L. Cederbaum, W. Gans (Eds.), Fractals, Quasicrystals, Chaos, Knots and Algebraic Quantum Mechanics, Kluwer, Dorbrecht, 1988, p. 21.

[15] B. Roling, Phys. Rev. B 61 (2000) 5993.

[16] V.M. Syutkin, Chem. Phys. 248 (1999) 213.

[17] G.P. Johari, J. Non-Cryst. Solids 307–310 (2002) 317.

[18] G.P. Johari, M. Goldstein, J. Chem. Phys. 55 (1971) 4245.